The Impact of Doping on the Anti-Resonance Effects of A_{1g}^1 Mode of InSe

Mahmoud Zolfaghari Department of Physics, University of Sistan and Baluchestan, Zahedan, Iran

Corresponding Author's Email: mzolfaghari@phys.usb.c.ir

Received: Mar. 15, 2018, Revised: May. 29, 2018, Accepted: Oct. 2, 2018, Available Online: Dec. 27, 2019

DOI: 10.29252/ijop.13.2.171

ABSTRACT– A comparative study of antiresonance effects in InSe and InSe doped with GaS, using the resonant Raman spectroscopy is presented. The nonpolar optical phonon of A^1_{lg} symmetry in InSe exhibits a pronounced decrease in the Raman cross-section at excitation energy 2.585 eV. In InSe doped with GaS samples, it is found that the anti-resonance behavior decreases as doping contents are increased. To account these observations, a model is applied to explain and interpret the Raman intensity evolution versus incident photon energy. The agreement between theory and experiment is good.

KEYWORDS: Anti-resonance; InSe; GaS; Raman scattering

I.Introduction

Low dimensional materials especially 2D materials are focus of recent research. This is to their promising applications; in nonlinear optics, sensors, optoelectronics devices, etc. at nanoscale compatible with Si. This follows from graphene as a genuine 2D material which is ideal for next generation application the mentioned in areas. Nevertheless, graphene presently suffers from technological shortage. In graphene, the conduction and the valence bands coincide at Fermi energy, so graphene is a zero bandgap semiconductor. This means that there are no electronic states in graphene that allow photoexcited carriers to be created to develop optoelectronic devices. [1, 2]. Moreover, despite of the high photo-response and responsivity of graphene, the dark current is high due to lack of bandgap [3-5]. This shortcoming of graphene acts as a catalyst to search for novel 2D material in the form of atomic layers of semiconductor materials [6].

In view of the above argument, the layered semiconducting material belonging to III-VI group have been examined for layered photoresponse materials [7-10]. Due to their nonlinear effect and good photo-response, these layered materials have been used generally in the area of nonlinear optics, photodetection and Terahertz generation source [11-14]. Synthetic few layers of GaSe [8] has demonstrated an external quantum efficiency and it's mechanically exfoliated [9, 15] has a good photo-response with low dark currents. Nevertheless, theoretical [16] as well as experimental works [8] have demonstrated that, the gap energy of GaSe changes from 1.8 eV with decreasing layers' number to a higher value 3.2 eV. This originates from the p_z-like orbitals of Se atoms that are suppressed from interlayer interactions [6]. This causes photoresponse of device to be weak in the visible light region. On the other hand, InSe having similar band structure to GaSe has a narrow bandgap [14, 17], which nearly overlaps perfectly the visible spectrum hence suitable for the above mentioned 2D layered materials

As one of the ways to reach the nanoscale is from top to down, therefore, a better understanding of these interesting layered material, e.g. InSe in bulk form, will be helpful in better understanding them in nanoscale size.

The InSe compound belongs to the III-VI family, each layer of InSe consists of four closed packed covalently bounded monatomic sheets in the sequence Se-In-In-Se. The binding of the atoms within the layer is strong and is covalent or ionic while individual layers are held together by relatively weaker van der Waal's forces. Due to the relatively weak interlayer interaction, layered crystals can be regarded as ensemble of sheets (layers) stack in the c direction. There are, in general, three possible positions for each layer (as in the hcp and fcc structures for the packing of spheres). Such few restrictions on the order of packing vield the stacking sequence of these identical unit layers which differs only in the stacking sequence of these layers. The different stackings are called polytype. The different stacking sequence of the layers in the III-VI family are ε , β , and γ -polytypes.

As a result of the nature of the interaction described above, these materials are highly anisotropic in their physical properties and easy cleavage in plane perpendicular to the c axis.

The γ -InSe modification belongs to the space group $C_{3v}^5(R3)$. The rhombohedral unit cell of the γ -InSe (Fig. 1) contains only two molecules of InSe [18]. The (a, b) plane is parallel to the layers and this plane is tilled at 150° from the c axis. In the trigonal representation a=b=0.4002 nm, c=0.875nm, $\alpha=30^{\circ}$, $\gamma=105^{\circ}$ and $\theta=29^{\circ}$. The main atoms' distances are In-In =0.282 nm, Se-Se=0.386 nm. The van der Waals gap width is 0.305 nm. The lowest direct and indirect bandgap in InSe at 300 K are at 1.256 and 1.187 eV, respectively [19]. The energy of the hyperbolic exciton near the M₁ saddle point is 2.77 eV at 300 K. The normal modes of vibration are represented as, $\Gamma = 4 \Gamma_1(A_1) + 4\Gamma_3(E)$ which one Γ_1 and one Γ_3 are acoustic modes and others are optical modes. All optical modes are Raman and IR active.

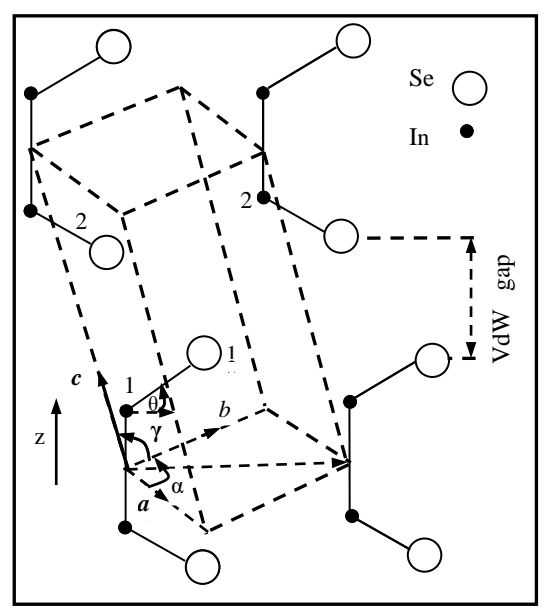


Fig. 1. Unit cell representation of γ -InSe. In the trigonal representation a=b=0.4002 nm, c=0.875 nm, $\alpha=30^\circ$, $\gamma=105^\circ$ and $\theta=29^\circ$. The main atoms' distances are In-In=0.282 nm, Se-Se=0.386 nm. The van der Waals gap width is 0.305 nm.

Raman scattering is a powerful technique for probing lattice vibration [18-27, 30-33], resonance Raman scattering (RRS) [18, 24] and anti-resonance effect [26] in the layered semiconductor materials. Numerous researchers have studied anti-resonance effects for CdS semiconductor [25, 26] and have found that cancellation of scattering amplitude occurs near 2.41 eV. Similar study has been conducted for GaSe layered compound [27]. Weszka et al.[30-32] have studied temperature dependence Raman scattering and RRS of amorphous indium selenide film. From optical phonon in InSe at 2 K, Kuroda and Nishina [18, 20-22] have measured RRS and attributed the resonance enhancement to the exciton energy E_1 at 2.531 eV at 77 K [18, 20]. Ashokan et al. [23] have formulated theory of RRS in a quasi-two-dimensional InSe near excitonic transition. Zolfaghari et al. have studied the effect of doping of InSe with GaS in a systematic way [24]. They found that as a result of GaS doping InSe: (i) there is a shift in the excitonic energy E_1 toward higher energy values, (ii) all modes exhibit broadening indicating topological disorder. (iii) At room temperature, the Raman spectrum of InSe doped with GaS displays the off-resonance behavior with laser excitation energy of 2.41 eV and at 77 K, it shows resonance enhancement with laser excitation energy of 2.54 eV.

In this report, the anti-resonance behavior of nonpolar A_{lg} (116 cm⁻¹) mode of pure InSe and InSe doped with GaS which was observed previously will be discussed [24].

II. THEORETICAL BACKGROUND

In Raman scattering when the photon energy approaches the energy gap $E_{\rm g}$ or excitonic transition in InSe an enhancement in the Raman scattering efficiency is observed. However, in some materials, pronounced decrease in Raman scattering efficiency is observed, before the onset of resonance Raman enhancement [25-27]. In InSe, a monotonic decrease in scattering efficiency of nonpolar optical mode of A_{1g}^1 symmetry (116 cm⁻¹) is observed as photon energy approaches excitonic energy [24]. This decrease in the Raman scattering cross-section is referred to as anti-resonance [26]. Although fairly detailed cross-section analysis of $\,A^{\scriptscriptstyle 1}_{\scriptscriptstyle 1g}\,$ phonon has been carried out, the peculiarities of decrease in A_{1g}^{1} symmetry phonon cross section have not been investigated quantitatively.

Kuroda and Nishina have also observed this behavior in their investigation of resonant Raman scattering at M_0 edge (hydrogenic exciton) of InSe [18]. To account for this behavior theoretically, they used Raman tensor of nonpolar phonon at the isotropic M_0 exciton edge given by Zeyher *et al.* [28]. The expression for resonant Raman tensor at the M_0 exciton is given [18, 28]:

$$R(\omega) = \frac{A}{\pi a_0^3} \left\{ \sum_{n=1}^{\infty} \frac{1}{n^3} \times \frac{1}{\left[\hbar \omega + i \eta_D + \frac{E_B}{n^2} - E_g\right] \left[\hbar \omega' + i \eta_D + \frac{E_B}{n^2} - E_g\right]} + \frac{1}{\left[\hbar \omega + i \eta_D + \frac{E_B}{n^2} - E_g\right]} + \frac{1}{\left[\hbar \omega + i \eta_D + \frac{E_B}{n^2} - E_g\right]} + \frac{1}{\left[\hbar \omega + i \eta_D + \frac{E_B}{n^2} - E_g\right]} + \frac{1}{\left[\hbar \omega + i \eta_D + \frac{E_B}{n^2} - E_g\right]} + \frac{1}{\left[\hbar \omega + i \eta_D + \frac{E_B}{n^2} - E_g\right]} + \frac{1}{\left[\hbar \omega + i \eta_D + \frac{E_B}{n^2} - E_g\right]} + \frac{1}{\left[\hbar \omega + i \eta_D + \frac{E_B}{n^2} - E_g\right]} + \frac{1}{\left[\hbar \omega + i \eta_D + \frac{E_B}{n^2} - E_g\right]} + \frac{1}{\left[\hbar \omega + i \eta_D + \frac{E_B}{n^2} - E_g\right]} + \frac{1}{\left[\hbar \omega + i \eta_D + \frac{E_B}{n^2} - E_g\right]} + \frac{1}{\left[\hbar \omega + i \eta_D + \frac{E_B}{n^2} - E_g\right]} + \frac{1}{\left[\hbar \omega + i \eta_D + \frac{E_B}{n^2} - E_g\right]} + \frac{1}{\left[\hbar \omega + i \eta_D + \frac{E_B}{n^2} - E_g\right]} + \frac{1}{\left[\hbar \omega + i \eta_D + \frac{E_B}{n^2} - E_g\right]} + \frac{1}{\left[\hbar \omega + i \eta_D + \frac{E_B}{n^2} - E_g\right]} + \frac{1}{\left[\hbar \omega + i \eta_D + \frac{E_B}{n^2} - E_g\right]} + \frac{1}{\left[\hbar \omega + i \eta_D + \frac{E_B}{n^2} - E_g\right]} + \frac{1}{\left[\hbar \omega + i \eta_D + \frac{E_B}{n^2} - E_g\right]} + \frac{1}{\left[\hbar \omega + i \eta_D + \frac{E_B}{n^2} - E_g\right]} + \frac{1}{\left[\hbar \omega + i \eta_D + \frac{E_B}{n^2} - E_g\right]} + \frac{1}{\left[\hbar \omega + i \eta_D + \frac{E_B}{n^2} - E_g\right]} + \frac{1}{\left[\hbar \omega + i \eta_D + \frac{E_B}{n^2} - E_g\right]} + \frac{1}{\left[\hbar \omega + i \eta_D + \frac{E_B}{n^2} - E_g\right]} + \frac{1}{\left[\hbar \omega + i \eta_D + \frac{E_B}{n^2} - E_g\right]} + \frac{1}{\left[\hbar \omega + i \eta_D + \frac{E_B}{n^2} - E_g\right]} + \frac{1}{\left[\hbar \omega + i \eta_D + \frac{E_B}{n^2} - E_g\right]} + \frac{1}{\left[\hbar \omega + i \eta_D + \frac{E_B}{n^2} - E_g\right]} + \frac{1}{\left[\hbar \omega + i \eta_D + \frac{E_B}{n^2} - E_g\right]} + \frac{1}{\left[\hbar \omega + i \eta_D + \frac{E_B}{n^2} - E_g\right]} + \frac{1}{\left[\hbar \omega + i \eta_D + \frac{E_B}{n^2} - E_g\right]} + \frac{1}{\left[\hbar \omega + i \eta_D + \frac{E_B}{n^2} - E_g\right]} + \frac{1}{\left[\hbar \omega + i \eta_D + \frac{E_B}{n^2} - E_g\right]} + \frac{1}{\left[\hbar \omega + i \eta_D + \frac{E_B}{n^2} - E_g\right]} + \frac{1}{\left[\hbar \omega + i \eta_D + \frac{E_B}{n^2} - E_g\right]} + \frac{1}{\left[\hbar \omega + i \eta_D + \frac{E_B}{n^2} - E_g\right]} + \frac{1}{\left[\hbar \omega + i \eta_D + \frac{E_B}{n^2} - E_g\right]} + \frac{1}{\left[\hbar \omega + i \eta_D + \frac{E_B}{n^2} - E_g\right]} + \frac{1}{\left[\hbar \omega + i \eta_D + \frac{E_B}{n^2} - E_g\right]} + \frac{1}{\left[\hbar \omega + i \eta_D + \frac{E_B}{n^2} - E_g\right]} + \frac{1}{\left[\hbar \omega + i \eta_D + \frac{E_B}{n^2} - E_g\right]} + \frac{1}{\left[\hbar \omega + i \eta_D + \frac{E_B}{n^2} - E_g\right]} + \frac{1}{\left[\hbar \omega + i \eta_D + \frac{E_B}{n^2} - E_g\right]} + \frac{1}{\left[\hbar \omega + i \eta_D + \frac{E_B}{n^2} - E_g\right]} + \frac{1}{\left[\hbar \omega + i \eta_D + \frac{$$

$$\frac{1}{4\hbar\omega_{0}E_{B}}\left[\ln\left|\frac{\hbar \ \omega'+i\,\eta_{C}\ -E_{g}}{\hbar \ \omega+i\,\eta_{C}\ -E_{g}}\right|+i\left[\tan^{-1}\left(\frac{\hbar\omega-E_{g}}{\hbar\eta_{C}}\right)-\tan^{-1}\left(\frac{\hbar\omega'-E_{g}}{\hbar\eta_{C}}\right)+\pi \ \coth z\left(\omega\right)-\coth z\left(\omega'\right)\right]\right]\right\}$$
(1)

with

$$\begin{split} z\left(\omega\right) &= \pi \sqrt{\frac{E_{B}}{\hbar \ \omega + i \ \eta_{c} \ -E_{g}}} \\ &= \pi \alpha e^{-i\theta} \quad \text{if} \quad \hbar \omega - E_{g} \geq 0 \\ &= \pi \alpha e^{-i\left(\theta + \frac{\pi}{2}\right)} \quad \text{if} \quad \hbar \omega - E_{g} < 0, \end{split}$$

and

$$\alpha(\omega) = \pi \left(\frac{E_B}{\sqrt{\hbar \omega - {E_g}^2 + \hbar (\eta_c)^2}} \right)^{1/2},$$

$$\theta(\omega) = \frac{1}{2} \tan^{-1} \left(\frac{\hbar \eta_C}{\hbar \omega - E_g} \right).$$

where $\hbar\omega$, $\hbar\omega'$, and $\hbar\omega_0$ are energies of incident photons, scattered photons and respectively, E_B and a_0 the emitted phonons binding energy and Bohr radius respectively of the first exciton. The constant E_g is the energy gap, while $\eta_{\scriptscriptstyle D}$ and $\eta_{\scriptscriptstyle C}$ are phenomenological damping constants of the discrete and continuum exciton levels, respectively. The constant A is the coefficient which involves momentum matrix element. exciton-phonon deformation potential, and other fundamental constants.

Equation (1) used by Kuroda and Nishina to compare the experimentally observed results with the theory [18]. They found that there is a good agreement between theory and experimental results can only be obtained below the exciton energy while above the exciton edge there is a deviation between theory and experiment. They extended their study and used the two dimensional hydrogenic exciton

proposed by Jain and Choudhury [29] and again found unsatisfactory results for their data. Eventually, they gave no further consideration [18].

III. RESULTS

Single crystals of InSe and InSe doped with different GaS dopant concentrations from 0.7, 2.5, 10, and 100 ppm were grown using the modified Bridgman technique. This method provides crystals having the γ modification with a rhombohedral (R3) structure [34, 35]. the crystal preparation, details of experimental setup, and its geometry see Ref. [24] and for chemical analysis see Refs. [34, 35]. For a report of precipitation of impurity atoms that remain in the form of interlayer planes, see Ref. [36]. In this work results, for samples with GaS dopant concentrations of 2.5 and 100 ppm are presented.

Figure 2(a) shows a typical room temperature Raman scattering of pure InSe using incident photon energy of 2.54 eV, the main features are seen at 116, 177, and 226 cm⁻¹. This is in line with earlier reported Raman spectra of InSe [18, 20-24]. On decreasing temperature to 180 K, the Raman modes shift toward higher wavenumber with significant change in linewidth. In addition, the polar modes appear at 201 and 209 cm⁻¹ and the nonpolar modes position shifts from 116 to 117 cm⁻¹, 177 to 179 cm⁻¹ and 226 to 230 cm⁻¹. At 140 K, the intensity of the nonpolar Alg mode decreases and becomes very weak and the polar mode at 209 cm⁻¹ shifts to 211 cm⁻¹ as can be seen in Fig. 2(c). As the temperature is further lowered to 77 K, the very weak nonpolar A_{1g}^{1} mode appears with a peak at A11g is not inline, and enhancement in the Raman intensity is observed. At the same time, the intensity of the Rayleigh tail increases which is probably due to the intense resonant luminescence of the E_1 exciton. The Raman intensity of all modes remains unchanged as temperature further decreases to 20 K.

The enhancement in the Raman intensity and appearance of the polar modes at low temperature can be understood if one considers the band gap temperature dependence of pure InSe. The temperature coefficient $\Delta E/\Delta T$ of energy gap of InSe is about -5.3×10⁻⁴ eV K⁻¹ in the temperature range 300-90 K [37]. With decrease in temperature, the laser excitation energy of 2.54 eV comes close to the exciton energy E_1 and remains almost in resonance from 77 K and down to 20 K for pure InSe [20], since in the temperature range 90-15 K, the temperature coefficient $\Delta E/\Delta T$ is much smaller, about -2×10^{-4} eV K⁻¹ [37]. As the laser excitation energy of 2.54 eV approaches the exciton energy E_1 on tuning temperature, the Raman scattering increases rapidly as shown in Fig. 2. New pair of lines appear at 201 and 209 cm⁻¹. At 77 K, the Raman intensity becomes highest due to resonance with exciton energy. Further decrease in the temperature does not affect the Raman intensity very much. Fig. 2, also shows that the phonons shift toward higher wave numbers on decreasing the temperature.

From the resonant Raman measurements and infrared measurements, the bands at about 201 and 209 cm⁻¹ are attributed to LO phonons which corresponds to A and E type mode in γpolytype, respectively [38]. The features at 201 and 209 cm⁻¹ are observed only nearresonance, whereas nonpolar modes are allowed by selection rules in the off-resonance condition. InSe is a polar semiconductor and the experimental results reveal that the polar modes are present only near-resonance, whereas nonpolar modes are allowed by selection rules in the off-resonance condition. At 77 K, the 2.54 eV laser excitation energy is near the exciton energy E_1 . Therefore, we observe the polar as well as the nonpolar modes in the Raman spectrum as shown in Fig. 2 (d).

A similar series of experiments were performed on InSe doped with GaS samples using excitation photon energy of 2.54 eV of argon-ion laser to ascertain the effect of increasing concentration of GaS. It is found

that the Raman intensity of $A_{\rm lg}^1$ mode increases when dopant concentration increases from 0.7 to 100 ppm, at temperature 140 K which indicates that the anti-resonance effect decreases with increasing dopant concentration.

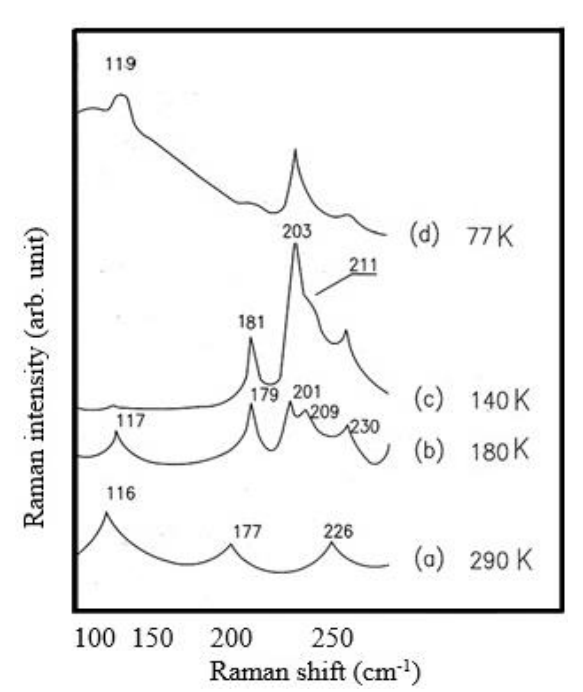


Fig. 2. One-phonon Raman spectrum of InSe at different temperatures recorded with excitation energy 2.54 eV of an argon ion laser. Spectrum (d) is compressed by 100 in order to bring it in proportionality to the other spectra.

IV. DISCUSSION

The Raman intensity variation of the A_{1g}^1 symmetry mode with temperature can be seen in Fig. 2. One of the most striking observations is anti-resonance effect. On decreasing the temperature from room temperature, the intensity of A_{1g} symmetry phonon mode starts decreasing and we observe a very weak intensity at 140 K as shown in Fig. 2(c). The Raman intensity never vanishes completely. The intensity of this mode starts increasing when the temperature is further decreased. In contrast to this effects, the Raman intensity of all other modes increases monotonically as resonance condition is approached. This decrease in the Raman scattering efficiency of A_{lg}^{1} mode can be observed in the following

experimental conditions: (i) by increasing the incident photon energy (from 2.41 to 2.71 eV) for a fixed temperature, (ii) by decreasing the temperature for fixed excitation photon energy.

more careful consideration of the experimental results by RRS studies showed a pronounced dip in the Raman efficiency after the resonant enhancement. That is, pure InSe shows an anti-resonance effect above the gap energy, near excitation energy of 2.60 eV, and efficiency of the scattering A_{1g}^{1} mode decreases monotonically and then starts increasing. As already mentioned, Kuroda et al. have also observed the same effect [18]. Their theoretical fit to the experimental data is good only below 2.585 eV and theory deviates from experimental results above 2.585 eV (See Fig. 1 of [18]).

The anti-resonance effect has also been reported for nonpolar modes in CdS [25, 26]. This reduction in the Raman amplitude seems to contradict existing theories that predict a rise in the Raman amplitude. It was suggested that the observed anti-resonance (minima) is due to the neglect of the non-resonant terms in Loudon's theory. Therefore, a simple extension to include these neglected nonresonant terms previously, along with the usual resonant terms in the Raman scattering amplitude could account for the observed dispersion Raman modes [25].

Loudon has shown that for first-order Raman scattering which proceeds via electronradiation; electron-lattice interaction, third order time-dependent perturbation theory yields six terms in the Raman tensor, see Eq. (14) Ref. [39]. Ralston et al. isolated terms which possess a double-order divergence as the laser photon energy approaches this energy gap, and called it the resonant term [25]. Damen et al. [26] have modified the resonant term given by Ralston et al. by ignoring the phonon energy in comparison $(\hbar\omega_g - \hbar\omega_I)$, and considered the remaining five terms as essentially independent of ω_1 and denote their sum as constant B. Their expression for the total Raman cross-section is given by:

$$\sigma \sim \left[\frac{A \, \omega_g^2}{\left(\omega_g - \omega_l \right)^2} + B \right]^2, \tag{2}$$

where A and B are negative or positive constant. The energies \hbar_{ω_g} and $\hbar\omega_l$ are gap and laser energy, respectively.

Using this expression, Damen *et al.* were able to give a qualitative fit to their experimental data for the E_2 (1) symmetry of optical mode of CdS [26]. Hoff et al. [27] have also observed anti-resonance effect in GaSe layered compound which shows similar behavior as observed for CdS [25, 26]. They found that the Eq. (2) does not give qualitative agreement between experimental observations for GaSe. This is because the anti-resonance observed in the GaSe sample is much closer to the band gap and much deeper than the one observed in CdS. Therefore, Eq. (2) gives an antiresonance which is much narrower than the dip observed in GaSe. However, in case of InSe, the anti-resonance is observed above the band gap contrary to the cases of CdS and GaSe.

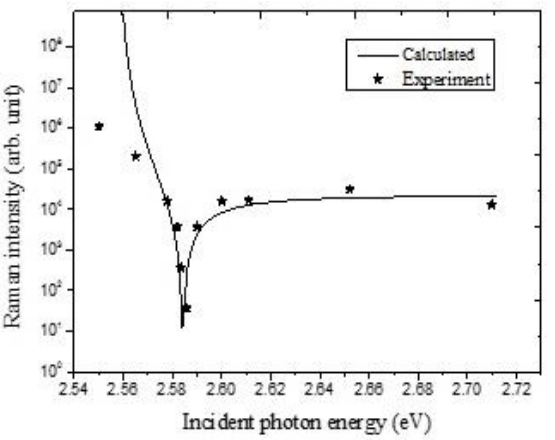


Fig. 3. Raman scattering cross section for A_{lg}^{l} optical phonon mode in InSe as a function of excitation energy at 20 K. The solid line is the theoretical calculation using Eq. (2) with $E_g = 2.558 \text{ eV}$.

To explain the experimental observations theoretically, Expression (2) has been used to calculate the Raman cross section for the nonpolar mode A_{1g}^1 at 20 K. The theoretical calculation (solid line) along with the experimental data is shown in Fig. 3. As can be seen, the agreement between theory and experiment is good. In this calculation, we obtained $B_9500|A|$ which leads to $\sigma \approx 0$ at $\hbar\omega \approx 2.585$ eV . By using the temperature coefficient of InSe, one obtains 2.54 eV which is equivalent to this excitation energy at 140 K which is in good agreement with the experiment.

Equation (2) of [18] (Eq. (1) in this report) has been used for the theoretical resonance behavior of Raman cross section for nonpolar mode A_{1g}^1 at 20 K for the M_0 exciton. Fig. 4 displays the calculated result in semilogarithmic scale. It is worthy of note that Fig. 4 shows only results for the samples of lowest and highest concentration of GaS dopant (i.e. 2.5 and 100 ppm) along with the experimental results of these two samples. The results for other two samples (i.e. for InSe doped with GaS (10 ppm) and InSe doped with GaS (20 ppm)) show behavior in between the results of the above mentioned samples. The antiresonance behavior for InSe doped with GaS (20 ppm) is less in comparison with InSe doped with GaS (10 ppm). As can be seen from Fig. 4, anti-resonance behavior decreases with increase in the dopant concentration. Fig. 4 also shows that the agreement between the theory and experiment is poor above 2.585 eV, because in the above theory, contribution of non-resonance terms have been ignored.

To the best of the author's knowledge, there is no anti-resonance theory for doped materials available in the literature. However, the experimental results in Fig. 4 show that cancellation between resonant and non-resonant term in the Raman amplitude is not the same as was the case for pure InSe.

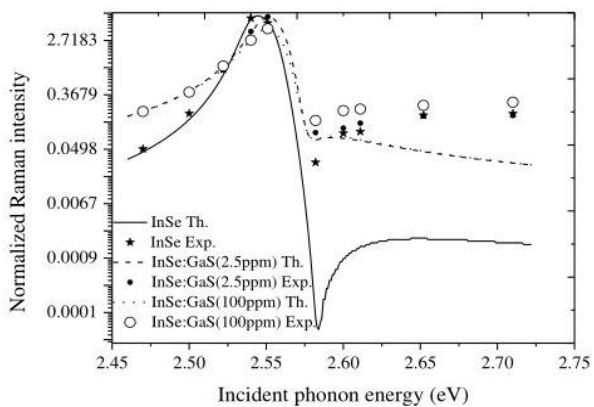


Fig. 4. Resonance curves for the 116 cm⁻¹ nonpolar mode at 20 K for InSe and various InSe:GaS doping densities. The Raman intensity is normalized with respect to 520 cm⁻¹ line of silicon and corrected for absorption. Solid lines are the curves obtained using Eq. (2) Ref.18, the discrete points are experimental points for InSe and InSe doped with GaS (2.5 ppm) and (100 ppm).

V. CONCLUSION

The nonpolar Raman-active A_{lg}^{l} phonon mode shows decrease in the Raman cross-section at excitation energy of 2.585 eV, analogous to that of the E_1 (1) (43 cm⁻¹) phonon in CdS. It was shown that the anti-resonance model based on Raman tensor given by Loudon and its modification by Daman *et al.* can explain the observed variation of the A_{lg}^{l} mode with temperature. Therefore, the inclusion of the non-resonant terms along with the resonant term in the Raman scattering amplitude appears to be important for proper theoretical fit of resonant Raman Effect in InSe type layered compounds.

A systematic study of variation of doping dependence on anti-resonance effect observed in Raman spectra of InSe doped with GaS carried out also. This is done by a comparative study of anti-resonance profile of several InSe samples doped with GaS with different concentrations. The results show decrease in anti-resonance behavior as dopant concentration is increased.

REFERENCES

[1] K. Dani, J. Lee, R. Sharma, A. Mohite, C. Galande, P. Ajayan, A. Dattelbaum, H. Htoon,

- A. Taylor, and R. Prasankumar. "Intraband conductivity response in Graphene observed using Ultrafast Infrared-Pump Visible-Probe Spectroscopy," Phys. Rev. B: Condens. Matt. Vol. 86, pp. 125403 (1-7), 2012.
- [2] S. Gilbertson, G.L. Dakovski, T. Durakiewicz, J.-X. Zhu, K.M. Dani, A.D. Mohite, A. Dattelbaum, and G. Rodriguez. "Tracing Ultrafast Separation and Coalescence of Carrier Distributions in Graphene with Time-Resolved Photoemission," J. Phys. Chem. Lett. Vol. 3, pp. 64–68, 2011.
- [3] B.Y. Zhang, T. Liu, B. Meng, X. Li, G. Liang, X. Hu, and Q. J. Wang "Broadband high photoresponse from pure Monolayer Graphene Photodetector," Nat. Commun. Vol. 4, pp. 1811 (1-11), 2013.
- [4] F. Xia, T. Mueller, Y.M. Lin, A. Valdes-Garcia, and P. Avouris. "Ultrafast Graphene Photodetector," Nat. Nanotechnol. Vol. 4, pp. 839–843, 2009.
- [5] T. Mueller, F. Xia, and P. Avouris. "Graphene photodetectors for high-speed optical communications," Nat. Photon. Vol. 4, pp. 297–301, 2010.
- [6] S. Lei, L. Ge, S. Najmaei, A. George, R. Kappera, J. Lou, M. Chhowalla, H.Yamaguchi, G. Gupta, R. Vajtai, A.D. Mohite, and P.M. Ajayan. "Evolution of the electronic band structure and efficient photodetection in atomic layers of InSe," ACS Nano. Vol. 8, pp. 1263–1272, 2014.
- [7] P. Hu, L. Wang, M. Yoon, J. Zhang, W. Feng, X. Wang, Z. Wen, J.C. Idrobo, Y. Miyamoto, D.B. Geohegan, and K. Xiao "Highly responsive ultrathin GaS nanosheet rigid photodetectors on and flexible substrates," Nano Lett. Vol. 13, pp. 1649-1654, 2013.
- [8] S. Lei, L. Ge, Z. Liu, S. Najmaei, G. Shi, G. You, J. Lou, R. Vajtai, and P.M. Ajayan. "Synthesis and photo response of large GaSe atomic layers," Nano Lett. Vol. 13, pp. 2777–2781, 2013.
- [9] P. Hu, Z. Wen, L. Wang, P. Tan, and K. Xiao. "Synthesis of few-layer GaSe nanosheets for high performance photodetectors," ACS Nano. Vol. 6, pp. 5988–5994, 2012.
- [10] M. Lin, D. Wu, Y. Zhou, W. Huang, W. Jiang, W. Zheng, S. Zhao, C. Jin, Y. Guo, H. Peng, and Zh. Liu "Controlled growth of atomically

- thin In₂Se₃ flakes by van der Waals epitaxy," J. Am. Chem. Soc. Vol. 135, pp. 13274–13277, 2013.
- [11] W. Shi, Y. J. Ding, N. Fernelius, and K. Vodopyanov. "Efficient, tunable, and coherent 0.18-5.27-THz source based on GaSe crystal," Erratum. Opt. Lett. Vol. 28, pp. 136–136, 2003.
- [12] K.R. Allakhverdiev, M.Ö. Yetis, S. Özbek, T. K. Baykara, and E.Y. Salaev. "Effective nonlinear GaSe crystal, optical properties and applications," Laser Phys. Vol. 19, pp. 1092–1104, 2009.
- [13] C. Kübler, R. Huber, S. Tübel, and A. Leitenstorfer. "Ultrabroadband detection of multi-terahertz field transients with GaSe electro-optic sensors: approaching the Near Infrared," Appl. Phys. Lett. Vol. 85, pp. 3360-3362, 2004.
- [14] A. Segura, J. Bouvier, M. Andrés, F. Manjón, and F.V. Munoz, "Strong optical nonlinearities in gallium and indium selenides related to inter-valence-band transitions induced by Light Pulses," Phys. Rev. B: Condens. Matt. Vol. 56, pp. 4075–4084, 1997.
- [15] D.J. Late, B. Liu, J. Luo, A. Yan, H.S. Matte, M. Grayson, C.N. Rao, and V.P. Dravid. "GaS and GaSe ultrathin layer transistors," Adv. Mater. Vol. 24, pp. 3549–3554, 2012.
- [16] D. V. Rybkovskiy, N. R. Arutyunyan, A. S. Orekhov, I. A. Gromchenko, I. V. Vorobiev, A. V. Osadchy, E. Y. Salaev, T. K. Baykara, K. R. Allakhverdiev, and E.D. Obraztsova. "Size-induced effects in gallium selenide electronic structure: The influence of interlayer interactions," Phys. Rev. B: Condens. Matt. Vol. 84, pp. 085314 (1-7), 2011.
- [17] O.Z. Alekperov, M.O. Godjaev, M.Z. Zarbaliev, and R.A. Suleimanov. "Interband photoconductivity in layer semiconductors GaSe, InSe and GaS," Solid State Commun. Vol. 77, pp. 65–67, 1991.
- [18] N. Kuroda and Y. Nishina. "Resonant Raman scattering at higher M_0 exciton Edge in layer compound InSe," Solid State Commun. Vol. 28, pp. 439-443, 1978.
- [19] S. Jand and J.L. Brebner. "Group theoretical analysis of lattice vibrations in GaSe polytypes," Can. J. Phys. Vol. 52, pp. 2454-2458, 1974.

- [20] N. Kuroda and Y. Nishina. "Directional dispersion of extraordinary phonons in layer compound InSe," Solid State Commun. Vol. 30, pp. 95-98, 1979.
- [21] N. Kuroda and Y. Nishina. "Resonance Raman scattering study on exciton and polaron anisotropies in InSe," Solid State Commun. Vol. 34, pp. 481-484, 1980.
- [22] N. Kuroda, I. Munakata, and Y. Nishina. "Exciton selection rules in the polarized resonant Raman scattering by LO phonons in InSe," J. Phys. Soc. Jpn. Vol. 51, pp. 839-843, 1982
- [23] S. Ashokan, K.P. Jain, M. Balkanski, and C. Julien. "Resonant Raman scattering in quasitwo-dimensional InSe near the M₀ and M₁ critical points," Phys. Rev. B. Vol. 44, pp. 11133-11142, 1991.
- [24] M. Zolfaghari, K.P. Jain, H.S. Mavi, M. Balkanski, C. Julien, and A. Chevy. "Raman investigation of InSe doped with GaS," Mater. Sci. Eng. B, Vol. 38, pp. 161-170, 1996.
- [25] J.M. Ralston, R.L. Wadsack, and R.K. Chang "Resonant cancelation of Raman scattering from CdS and Si," Phys. Rev. Lett. Vol. 25, pp. 814-818, 1970.
- [26] T.C. Damen and J.F. Scott. "Anti-resonance of Raman cross-sections for nonpolar phonons in CdS," Solid State Commun. Vol. 9, pp. 383-385, 1971.
- [27] R.M. Hoff and J.C. Irwin. "Resonant Raman scattering in GaSe," Phys. Rev. B, Vol. 10, pp. 3464-3470, 1974.
- [28] R. Zeyher, C.S. Ting and J.L. Birman. "Polariton theory of first-order Raman scattering in finite crystals for transparent and absorbing frequency regions," Phys. Rev. B, Vol. 10, pp. 1725-1740, 1974.
- [29] K.P. Jain and G. Choudhury." Resonant Raman scattering at the critical points of semiconductors," Phys. Rev. B. Vol. 8, pp. 676-681, 1973.
- [30] J. Weszka, Ph. Daniel, A.M. Burian, A. Burian, and M. Zelechower. "Resonance Raman scattering in In_{0.45}Se_{0.55} amorphous films," Solid State Commun. Vol. 118, pp. 97-102, 2001.
- [31] J. Weszka, Ph. Daniel, A. Burian, A.M. Burian, and A.T. Naguyen. "Raman scattering

- in In₂Se₃ and InSe₂ amorphous films," J. Non-Cryt. Solids, Vol. 265, pp. 98-108, 2000.
- [32] J. Weszka, Ph. Daniel, A.M. Burian, A. Burian, and M. Zelechower. "Temperature dependence of Raman scattering in amorphous films of In_{1-x}Se_x alloys," Solid State Commun. Vol. 119, pp. 533-537, 2001.
- [33] S. Marsillac, A.M. Combot-Marie, J.C. Bernede, and A. Conan. "Experimental evidence of the low-temperature formation of γ -In₂Se₃ thin films obtained by a solid-state reaction," Thin Solid Film, Vol. 288, pp. 14-20, 1996.
- [34] A. Chevy, Cristallogénèse et caractérisation du monoséléniure d'indium-conversion photovoltaïque de l'energie, PhD Thesis, , Universitè Pierre et Marie Curie, Paris 1981.
- [35] A. Chevy, A. Kuhn and M.S. Martin. "Large InSe monocrystals grown from A non-stoichiometric melt," J. Cryst. Growth. Vol. 38, pp. 118-123, 1977.
- [36] P. Houdy, Croissance, caractérisation, propriétés de matériaux pour cellules solaires, These de 3êam cycle, Universitè de Paris VII, 1982.
- [37] G.I. Abutalyboy and M.L. Belle, "Modulation spectrum and profile of the absorption line of hyperbolic excitons in indium selenide," Sov. Phys. Semicond. Vol. 8, pp. 1559-1562, 1975.

- [38] S. Nakashima, M. Hangyo, and A. Mitsuishi, in J. R. Durig (ed.) "Vibrational Spectroscopy of layered materials," Elsevier, Amsterdam, Vol. 14, in Vibrational Spectroscopy and Structures, P. 305-308, 1985.
- [39] R. Loudon, "Theory of the first-order Raman effect in crystals," Proc. R. Soc. Lond. A. Vol. 275, pp. 218-232, 1963.



Mahmoud Zolfaghari was born in Tehran and did his PhD in Solid state ionic in India, University of Delhi and IIT, Delhi. His thesis was entitled: "Laser Raman Spectroscopy of layered materials." Then he joined the University of Sistan and Baluchestn. Dr Zolfaghari has supervised the theses of many graduated students and has published several Journal and Conference Papers.

THIS PAGE IS INTENTIONALLY LEFT BLANK.